Nanoparticulate Anode

DOI: 10.1002/ange.201108300

Nanoparticulate TiO_2(B): An Anode for Lithium-Ion Batteries**

*Yu Ren, Zheng Liu, Frédérique Pourpoint, A. Robert Armstrong, Clare P. Grey, and Peter G. Bruce**

Titanates are being intensively investigated as anodes for lithium-ion batteries due to their superior safety and rate capability compared with graphite, although their higher voltage lowers the overall energy density of the lithium-ion cell.[1] $Li_4Ti_5O_{12}$ spinel is now used in commercial lithium-ion batteries.[2] TiO_2 possesses twice the theoretical specific capacity (335 mA h g^{-1}) compared with $Li_4Ti_5O_{12}$ (175 mA h g^{-1}), i.e., is comparable to graphite, rendering TiO_2 potentially attractive as an anode for Li-ion batteries.[1b–h,3] TiO_2(B) can accommodate more lithium than any other TiO_2 polymorph as a bulk material (micrometer-sized particles).[3e,4] It has been shown that nanostructured forms of TiO_2(B) enhance rate capability compared to the bulk, with nanotubes of TiO_2(B) or TiO_2(B)/anatase microspheres exhibiting the highest rate capability to date.[5] Their performance is exceeded by nanoparticulate TiO_2(B) described here.

Nanoparticulate TiO_2(B) was synthesized by a procedure described in the Experimental Section. Briefly, Ti metal is dissolved in a mixture of H_2O_2 and NH_3 in water, to which glycolic acid is added, forming a titanium glycolate complex. This is subjected to hydrothermal treatment at 160 °C for 30 min. The resulting solid was finally calcined in dry air at 300 °C for 1 h. The powder X-ray diffraction pattern (PXRD) of nanoparticulate TiO_2(B) is shown in Figure 1, where it is compared with standard TiO_2(B). The small particle dimensions necessarily result in peak broadening but the powder diffraction pattern follows the same intensity distribution as that of the bulk material. Confirmation that the nanoparticulate powder is TiO_2(B) was obtained by high-resolution TEM (Figure 2); lattice spacings of 0.357 nm and 0.619 nm corresponding to the (110) and (001) reflections from the TiO_2(B) structure (ICDD 046-1237) are observed. ^{17}O NMR spectra of ^{17}O-enriched TiO_2 clearly show characteristic resonances from the three oxygen coordination environments OTi_2, OTi_3, and OTi_4 in intensity ratios of approximately 1:2:1, which is characteristic of the TiO_2(B) polymorph (Supporting Information, Figure S2). Rutile and anatase both contain only OTi_3 environments.

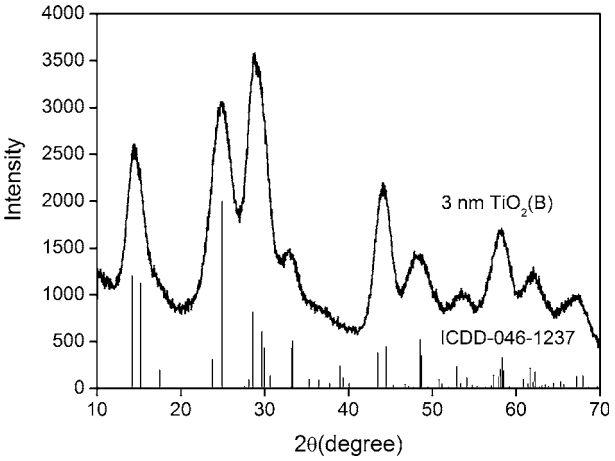

Figure 1. PXRD pattern of the TiO_2(B) nanoparticles. Bulk TiO_2(B) from the ICDD database is shown for comparison.

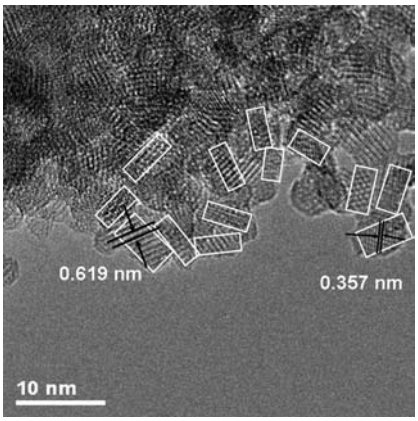

Figure 2. HRTEM image of TiO_2(B) nanoparticles. White boxes delineate primary (nano)particles within the agglomerates.

The TEM data demonstrate that the material is composed of nanoparticles of ca. 2.5 × 4.3 nm size (based on analysis of 100 nanoparticles), with a relatively narrow size distribution, and that form agglomerates of 0.3–3 μm (Figure 2a and S1). The BET surface area determined from N_2 adsorption is 251 $m^2 g^{-1}$ (pore volume 0.12 $cm^3 g^{-1}$) whereas, based on the primary particle size of 2.5 × 2.5 × 4.3 nm, the predicted surface area is 567 $m^2 g^{-1}$, i.e., more than twice the observed value and consistent with aggregation of the primary particles into porous agglomerates.

One problem that often besets nanoparticles is the need to employ molecules (e.g. surfactants) in the synthesis to inhibit particle size growth. Such molecules, if they remain on the

[*] Dr. Y. Ren, Z. Liu, Dr. A. R. Armstrong, Prof. P. G. Bruce
School of Chemistry, University of St Andrews
Purdie Building, North Haugh, St Andrews, KY16 9ST (UK)
E-mail: p.g.bruce@st-andrews.ac.uk
Dr. F. Pourpoint, Prof. C. P. Grey
Department of Chemistry, University of Cambridge (UK)

[**] P.G.B. and C.P.G. are indebted to the EPSRC including SUPERGEN and the programme grant "Nanoionics" for financial support and to EaStCHEM for a studentship for Y.R. C.P.G. and F.P. thank Dr. F. Blanc for help with the NMR spectroscopy.

Supporting information for this article is available on the WWW under http://dx.doi.org/10.1002/anie.201108300.

surface, may affect the properties of the material. Here, we have succeeded in removing the growth inhibiting molecules (glycolate) by calcining the nanoparticulate TiO_2(B) in air after hydrothermal treatment. CHN analysis of the calcined material indicates that the amount of residual carbon is 0.3 wt% which would account for a carbon layer of significantly less than 1 Å if distributed across the surface of the nanoparticles, i.e., the glycolate and any residue have been removed.

Nanoparticulate TiO_2(B) was incorporated into a composite electrode composed of Super P carbon and Kynar 2801 binder, then introduced into an electrochemical cell along with a lithium metal counter/reference electrode and liquid electrolyte. All procedures were carried out in an Ar-filled glovebox (H_2O and $O_2 < 1$ ppm). Further details of the electrode fabrication and cell assembly are given in the Experimental Section. The variation of cell voltage with Li content in nanoparticulate TiO_2(B) on the 1st, 2nd, 5th, 10th discharge (intercalation) then charge (deintercalation) are shown in Figure S3. The first discharge and charge capacities were 322 mA h g^{-1} and 247 mA h g^{-1}, respectively, indicative of an irreversible capacity loss on the first cycle. However, the second cycle efficiency has risen to 94%, and 98% after five cycles. Irreversible capacity loss in the first cycle with nanointercalation compounds is common and has been attributed to surface reactions with the electrolyte on reduction, something that has been discussed in detail for nanostructured TiO_2 previously[6] Once the surface layer has formed, the subsequent load curves correspond almost exclusively to lithium intercalation.

The load curves on the second cycle and the corresponding differential capacity plots (dQ/dV) for the TiO_2(B) nanoparticles are presented in Figure 3, where they are compared with the equivalent data for bulk, nanowire and nanotube TiO_2(B), the data for which were collected in previous studies.[5a] Some features of the electrochemistry for all four polymorphs are similar. All show a pair of plateaus in the load curves in the range 1.45–1.65 V. This is most clearly seen in the differential capacity plots (Figure 3b), where peaks correspond to plateaus in the load curves. Such plateaus indicate to the presence of two 2-phase intercalation processes. In the cases of the bulk and nanowire TiO_2(B) materials, diffraction data of sufficient quality to apply established methods of structure elucidation (Rietveld refinement) can be obtained and have been used previously to assign the 2-phase processes to intercalation into the A1 and A2 sites of the TiO_2(B) crystal structure.[7] Intercalation into the same sets of sites may be occurring in the nanotubes and nanoparticles but here the diffraction peaks are too broad to be analyzed by Rietveld refinement, rendering it difficult to determine definitively the Li site occupancies by neutron diffraction. The peaks in the differential capacity plots broaden and lower in intensity as the dimensions of the TiO_2(B) particles are reduced, indicative of a transformation from 2-phase reactions, with constant chemical potential, towards a system that exhibits a Li chemical potential which varies with overall Li content. This is commensurate with previous observations of intercalation compounds that exhibit a 2-phase intercalation process for large (bulk) particles but

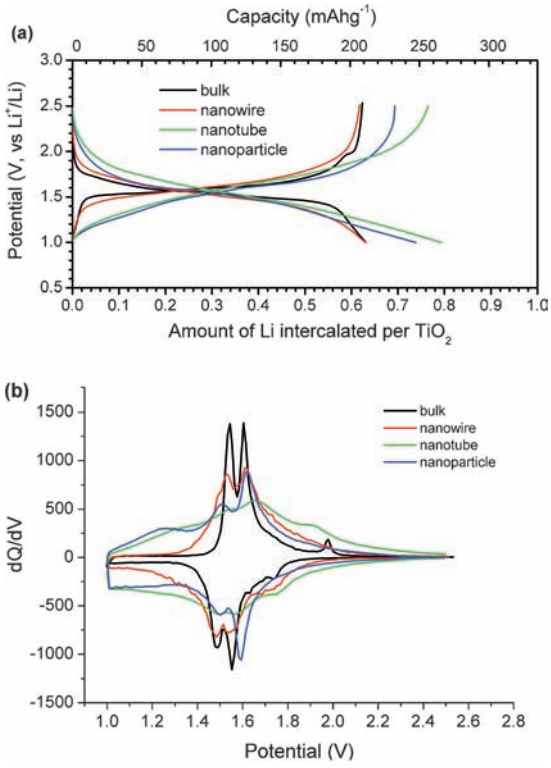

Figure 3. a) Variation of voltage with state-of-charge for discharge then charge of bulk TiO_2(B), TiO_2(B) nanowires, nanotubes, and nanoparticles on the second cycle and b) corresponding differential capacity plots. Rate 50 mA g^{-1}.

increasingly sloping load curves on reducing the particle dimensions.[1d,8]

Let us turn to the increased ability to store Li in the nanoparticles compare with the bulk. The dimensions of the nanoparticles are similar to the wall thickness of the nanotubes (2.5 nm), whereas the nanowires (35 nm × 2–10 μm) are much closer to the dimensions of the bulk particles (100 nm × 2 μm). The nanoparticles can accommodate more Li and hence store more charge (ca. 20%), even at low rates, than the bulk or nanowire morphologies (Figure 3), as noted previously for the TiO_2(B) nanotubes.[5a,9] The additional capacity appears mainly below 1.4 V and may be seen in the difference between the areas under the differential capacity plots in Figure 3b. The increased Li storage in nanoparticulate TiO_2(B) compared with bulk TiO_2(B) demonstrates that this is a general phenomenon due to reduced dimensions and not just observed in TiO_2(B) nanotubes. On reducing the dimensions of crystalline materials to the nanoscale a greater proportion of the material will be in the near surface region where it is subjected to different forces than in the bulk, resulting in structural distortions. Such distortions have been related to increased Li storage in TiO_2(B) nanotubes.[10] Similar structural distortions in the nanoparticles also exist but establishing them is challenging because the peaks in the diffraction pattern are too broad for Rietveld refinement, as noted above. Progress will require a combination of computer modeling (to generate trial structural distortions), NMR spectroscopy, and investigation of short-range structure with diffraction methods such as Debye and pair distribution

function (PDF) analysis. This study is underway and will form the basis of a future paper. Preliminary Debye analysis had already confirmed the nanoparticle morphology and size, as noted above. A very small peak is evident at around 1.20–1.35 V on oxidation in the case of the nanotubes and nanoparticles that does not appear in the TiO_2(B) materials of larger dimension, understanding its origin also requires a detailed knowledge of the structural distortions.

One other feature evident in the differential capacity plots is a reduction peak at around 1.75 V in the case of the bulk, nanowire, and nanotube morphologies, the first two of which also demonstrate an oxidation peak at around 1.90–2.00 V. Peaks around these voltages are observed in anatase and could signal a small degree of anatase contamination in the materials. However previous studies of bulk and nanowire TiO_2(B) using X-ray/neutron diffraction and Raman spectroscopy did not reveal any evidence for the presence of anatase and the peaks were interpreted as due to intercalation into the crystal structure of TiO_2(B).[7] It is noteworthy that these peaks appear to be absent in the case of the nanoparticles, which may be further evidence for the structural changes occurring with reduced dimensions.

A major driving force for the investigation of nanointercalation electrodes is to obtain the highest possible capacity to store charge (lithium) at high rates.[17] To explore the rate capability of the TiO_2(B) nanoparticles, it is first necessary to ensure that the electrochemistry within the range of rates studied is limited by the active material and not by the nature of the composite electrode (e.g. electrode thickness, proportion of carbon added). To ensure that this is the case, a series of composite electrodes were constructed with different proportions of carbon and separately different active mass loadings resulting in different overall thicknesses. The data are shown in Figure S4 and S5, from which we conclude that an electrode with the composition 70:20:10 (TiO_2:Super P:Kynar) and a mass loading of 3.5 mg cm^{-2} can be used to explore rates approaching 20000 mA g^{-1}.

The variation of gravimetric capacity (based on the active mass alone) with different charge/discharge rates is shown in Figure 4a, where the data of nanoparticulate TiO_2(B) are compared with several other titanate materials including nanoparticulate anatase (6 nm diameter), which correspond to the best previously reported rate capability of any titanate.[1g,11] The gravimetric capacity for the TiO_2(B) nanoparticles at all rates up to 18000 mA g^{-1} is almost identical to the 6 nm anatase particles, which have a much higher proportion of carbon (45 wt%, significantly more than the TiO_2(B) nanoparticles and corresponding to a mass loading of only 1.5 mg cm^{-2}) in their composite electrodes.

The effect of diluting the active material by a large amount of carbon (as in the case of the 6 nm anatase nanoparticles) is evident on examining the volumetric capacity (based on the total volume of the composite electrode) as a function of rate (Figure 4b). Nanoparticulate TiO_2(B) exhibits superior volumetric capacity at all rates compared with the 6 nm anatase material and the previously reported best high rate (> 1000 mA g^{-1}) volumetric capacity, namely mesoporous anatase. The relatively high volumetric capacity of the TiO_2(B) nanoparticles is in part due to the

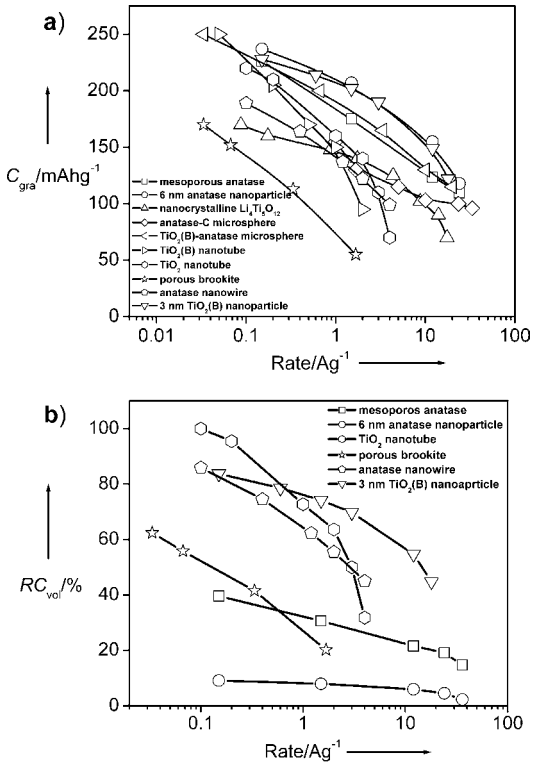

Figure 4. a) Gravimetric (C_{gra}) and b) relative volumetric capacity (RC_{vol}) retention of TiO_2(B) nanoparticles compared with other titanate materials as a function of rate. The volumetric capacities are expressed relative to the highest value for the anatase nanotubes (synthesized from $H_2Ti_2O_5{\cdot}H_2O$). For each electrode, the ratio of active material:carbon:binder is given in brackets. In the case of the data reported in Figure 4b, the composite electrode density is also given in brackets. Mesoporous anatase (square, 70:15:15, 0.50 g cm^{-3}),[11] 6 nm anatase nanoparticles (circle, 50:45:5, 0.15 g cm^{-3}),[1f,11] nanocrystalline $Li_4Ti_5O_{12}$ (triangle, 85:15:5),[12] 94% anatase/6%C microspheres (lozenge, 80:10:10),[13] 87% TiO_2(B)/13% anatase microspheres (left-pointing triangle, 70:15:15),[5b] TiO_2(B) nanotubes (right-pointing triangle, 75:18:7),[5a] TiO_2 nanotubes (anatase, from $H_2T_{i2}O_5{\cdot}H_2O$, hexagon, 75:15:10, 1.3 g cm^{-3}),[14] porous brookite (five-pointed star, 80:10:10 1.05 g cm^{-3}),[15] anatase nanowire (pentagon, 90:10:10, 1.3 g cm^{-3}),[16] and 3 nm TiO_2(B) nanoparticle (down-pointing triangle, 70:20:10, 1.05 g cm^{-3}). Only those materials for which electrode densities are available are presented in (b).

agglomerates formed by the primary nanoparticles, which helps to ensure a higher density of particles. The significance of this result is that maximizing volumetric capacity is at least as important as gravimetric capacity for future applications in lithium-ion cells.

In conclusion, TiO_2(B) nanoparticles with the smallest particle size yet reported (2.5 × 4.3 nm) have been synthesized. Their behavior as an intercalation host for Li has been explored and compared with other TiO_2(B) morphologies, specifically bulk, nanowires, and nanotubes. On reducing the dimensions from the bulk, through nanowires to nanotubes and nanoparticles, the amount of Li and hence charge that can be stored, even at low rates, increases with reduced dimensions. The two 2-phase intercalation processes, that are clearly present in bulk TiO_2(B) become less distinct and exhibit increasingly sloping load curves. The gravimetric capacity as a function of rate is almost identical to the previously

reported best performance for a titanate, which was for 6 nm anatase nanoparticles with very high carbon content in the composite electrode of 45 wt%. The volumetric capacity of composite electrodes with nanoparticulate TiO_2(B) is significantly higher than all previously reported titanate materials, including the 6 nm anatase nanoparticles, at rates above 1000 mA g^{-1}.

Experimental Section

TiO_2(B) nanoparticles were prepared using a hydrothermal method modified from a previously reported procedure.[18] In a typical synthesis, 0.72 g of Ti (99.7%, ≈325 mesh) was dissolved in an aqueous solution of H_2O_2 (70 mL, 30.0%) and NH_3 (20 mL, 35%) in an ice-water bath for 2–3 h with stirring. Then 1.71 g of glycolic acid (99%,) was dissolved in the solution, which was maintained at 80°C for several hours (3–4 h) to eliminate excess H_2O_2 and NH_3. The solution changed to a yellow gel. The gel was dissolved in ca. 40 mL of water to form a yellowish transparent solution. Upon addition of 3.0 g of H_2SO_4 (98.0%), the pH changed from 6 to 1. The total volume was then adjusted to 60 mL by adding water. The resulting solution were sealed in a Teflon-lined stainless steel autoclave and heated at 160°C for 30 min. After cooling to room temperature, the solid products were separated from the solutions by centrifugation, and washed several time by water and ethanol to remove the residue acid. Finally, the solid was dried at 60°C over night and calcined at 300°C for 1 h in dry air with a ramp rate of 1°C min^{-1}. The ^{17}O enriched TiO_2(B) nanoparticle for ^{17}O solid state NMR test was prepared with almost the same procedure as the above with two minor change: the amount of the material used for the synthesis is only 1/60 of the above example; ^{17}O-enriched H_2O (10 atom%, Euriso-Top, France) was used to hydrolyze the yellowish gel before the addition of H_2SO_4. The bulk TiO_2(B) was prepared according to a previous report.[7a] All the other chemicals used in the synthesis were purchased from Sigma–Aldrich and used as received. The 6 nm anatase nanoparticles were supplied by Tayca Corp., Japan.

The materials were characterized by TEM (JEOL JEM-2110), wide-angle PXRD (Stoe STADI/P diffractometer operating in transmission mode with Fe $K_{\alpha 1}$ radiation, $\lambda = 1.936$ Å), and N_2 adsorption (Micromeritics Tristar 3020).

Electrochemical cells were constructed by mixing the active material (TiO_2), Kynar 2801(a copolymer based on poly(vinylidene fluoride)), and Super P carbon (MMM) in the weight ratio of 70:20:10 if not otherwise specified. The mixture was cast onto copper foil from acetone using the Doctor-Blade technique. After solvent evaporation at room temperature and heating at 80°C under vacuum for 8 h, the electrodes were assembled into cells with a lithium electrode (99.9%, Aldrich) and LP-30 electrolyte (Merck; 1M $LiPF_6$ in 1:1 v/v ethylene carbonate/dimethyl carbonate). The cells were constructed and handled in an argon-filled MBraun glovebox. Electrochemical measurements were carried out using a MACCOR Series 4200 cycler. The electrode volume is obtained directly by measuring the electrode thickness and knowing the electrode area.

Received: November 24, 2011
Published online: January 17, 2012

Keywords: anodes · lithium-ion batteries · nanoparticles · titanium dioxide · volumetric capacity

[1] a) K. M. Colbow, J. R. Dahn, R. R. Haering, *J. Power Sources* **1989**, *26*, 397; b) I. Plitz, A. DuPasquier, F. Badway, J. Gural, N. Pereira, A. Gmitter, G. G. Amatucci, *Appl. Phys. A* **2006**, *82*, 615; c) E. Ferg, R. J. Gummow, A. Dekock, M. M. Thackeray, *J. Electrochem. Soc.* **1994**, *141*, L147; d) Y. G. Guo, Y. S. Hu, W. Sigle, J. Maier, *Adv. Mater.* **2007**, *19*, 2087; e) T. Ohzuku, A. Ueda, N. Yamamoto, *J. Electrochem. Soc.* **1995**, *142*, 1431; f) G. Sudant, E. Baudrin, D. Larcher, J. M. Tarascon, *J. Mater. Chem.* **2005**, *15*, 1263; g) C. H. Jiang, M. D. Wei, Z. M. Qi, T. Kudo, I. Honma, H. S. Zhou, *J. Power Sources* **2007**, *166*, 239; h) K. Amine, I. Belharouak, Z. Chen, T. Tran, H. Yumoto, N. Ota, S.-T. Myung, Y.-K. Sun, *Adv. Mater.* **2010**, *22*, 3052.

[2] a) A. Du Pasquier, C. C. Huang, T. Spitler, *J. Power Sources* **2009**, *186*, 508; b) T. Tan, H. Yumoto, D. Buck, B. Fattig, C. Hartzog, *The World Electric Vehicle Journal* **2007**, *2*, 76.

[3] a) P. Reale, S. Panero, B. Scrosati, *J. Electrochem. Soc.* **2005**, *152*, A1949; b) M. Wagemaker, W. J. H. Borghols, F. M. Mulder, *J. Am. Chem. Soc.* **2007**, *129*, 4323; c) W. J. H. Borghols, M. Wagemaker, U. Lafont, E. M. Kelder, F. M. Mulder, *Chem. Mater.* **2008**, *20*, 2949; d) L. Kavan, J. Prochazka, T. M. Spitler, M. Kalbac, M. T. Zukalova, T. Drezen, M. Gratzel, *J. Electrochem. Soc.* **2003**, *150*, A1000; e) D. Deng, M. G. Kim, J. Y. Lee, J. Cho, *Energy Environ. Sci.* **2009**, *2*, 818.

[4] A. R. Armstrong, G. Armstrong, J. Canales, P. G. Bruce, *Angew. Chem.* **2004**, *116*, 2336; *Angew. Chem. Int. Ed.* **2004**, *43*, 2286.

[5] a) G. Armstrong, A. R. Armstrong, J. Canales, P. G. Bruce, *Electrochem. Solid-State Lett.* **2006**, *9*, A139; b) H. Liu, Z. Bi, X.-G. Sun, R. R. Unocic, M. P. Paranthaman, S. Dai, G. M. Brown, *Adv. Mater.* **2011**, *23*, 3450.

[6] a) P. Poizot, S. Laruelle, S. Grugeon, L. Dupont, J. M. Tarascon, *Nature* **2000**, *407*, 496; b) Q. Wang, Z. Wen, J. Li, *Inorg. Chem.* **2006**, *45*, 6944; c) Y. S. Hu, L. Kienle, Y. G. Guo, J. Maier, *Adv. Mater.* **2006**, *18*, 1421; d) C. H. Jiang, I. Honma, T. Kudo, H. S. Zhou, *Electrochem. Solid-State Lett.* **2007**, *10*, A127; e) W. J. H. Borghols, D. Lutzenkirchen-Hecht, U. Haake, W. Chan, U. Lafont, E. M. Kelder, E. R. H. van Eck, A. P. M. Kentgens, F. M. Mulder, M. Wagemaker, *J. Electrochem. Soc.* **2010**, *157*, A582; f) S. Brutti, V. Gentili, P. Reale, L. Carbone, S. Panero, *J. Power Sources* **2011**, *196*, 9792.

[7] a) A. R. Armstrong, C. Arrouvel, V. Gentili, S. C. Parker, M. S. Islam, P. G. Bruce, *Chem. Mater.* **2010**, *22*, 6426; b) L. Brohan, R. Marchand, *Solid State Ionics* **1983**, *9–10*, 419.

[8] a) P. Gibot, M. Casas-Cabanas, L. Laffont, S. Levasseur, P. Carlach, S. Hamelet, J.-M. Tarascon, C. Masquelier, *Nat. Mater.* **2008**, *7*, 741; b) N. Meethong, H. Y. S. Huang, W. C. Carter, Y. M. Chiang, *Electrochem. Solid-State Lett.* **2007**, *10*, A134; c) G. Kobayashi, S.-i. Nishimura, M.-S. Park, R. Kanno, M. Yashima, T. Ida, A. Yamada, *Adv. Funct. Mater.* **2009**, *19*, 395; d) L. J. Hardwick, M. Holzapfel, P. Novak, L. Dupont, E. Baudrin, *Electrochim. Acta* **2007**, *52*, 5357.

[9] G. Armstrong, A. R. Armstrong, J. Canales, P. G. Bruce, *Chem. Commun.* **2005**, 2454.

[10] Y. G. Andreev, P. G. Bruce, *J. Am. Chem. Soc.* **2008**, *130*, 9931.

[11] Y. Ren, L. J. Hardwick, P. G. Bruce, *Angew. Chem.* **2010**, *122*, 2624; *Angew. Chem. Int. Ed.* **2010**, *49*, 2570.

[12] A. S. Prakash, P. Manikandan, K. Ramesha, M. Sathiya, J. M. Tarascon, A. K. Shukla, *Chem. Mater.* **2010**, *22*, 2857.

[13] F.-F. Cao, X.-L. Wu, S. Xin, Y.-G. Guo, L.-J. Wan, *J. Phys. Chem. C* **2010**, *114*, 10308.

[14] H. Kim, M. G. Kim, T. J. Shin, H.-J. Shin, J. Cho, *Electrochem. Commun.* **2008**, *10*, 1669.

[15] D. Dambournet, I. Belharouak, K. Amine, *Chem. Mater.* **2010**, *22*, 1173.

[16] M. G. Kim, H. Kim, J. Cho, *J. Electrochem. Soc.* **2010**, *157*, A802.

[17] a) P. G. Bruce, B. Scrosati, J. M. Tarascon, *Angew. Chem.* **2008**, *120*, 2972; *Angew. Chem. Int. Ed.* **2008**, *47*, 2930; b) M. S. Whittingham, *Dalton Trans.* **2008**, 5424; c) F. Cheng, Z. Tao, J. Liang, J. Chen, *Chem. Mater.* **2008**, *20*, 667; d) Y. G. Guo, J. S. Hu, L. J. Wan, *Adv. Mater.* **2008**, *20*, 2878.

[18] M. Kobayashi, V. V. Petrykin, M. Kakihana, *Chem. Mater.* **2007**, *19*, 5373.

